IOP Publishing Physica Scripta
Phys. Scr. **T151** (2012) 014021 (6pp) doi:10.1088/0031-8949/2012/T151/014021

Directed transport in coupled noisy Josephson junctions controlled via ac signals

L Machura, J Spiechowicz and J Łuczka

Institute of Physics, University of Silesia, Katowice, Poland

E-mail: jerzy.luczka@us.edu.pl

Received 26 March 2012
Accepted for publication 27 June 2012
Published 30 November 2012
Online at stacks.iop.org/PhysScr/T151/014021

Abstract
The transport properties of two coupled Josephson junctions driven by ac currents and thermal fluctuations are studied with the purpose of determining dc voltage characteristics. It is a physical realization of the directed transport induced by a non-biased zero averaged external signal. The ac current either (A) is applied to only one junction as a biharmonic current or (B) is split into two simple harmonic components and separately applied to the respective junctions. We identify the regimes where junctions can operate with the same as well as opposite signs of voltages. A general observation is that in the same parameter regime, scenario (B) is more efficient in the sense that the induced dc voltages take greater values.

PACS numbers: 05.60.−k, 74.50.+r, 85.25.Cp, 05.40.−a

(Some figures may appear in colour only in the online journal)

1. Introduction

Noisy transport in periodic arrangements [1] is widely present nowadays in many branches of science—in physics, biology, chemistry, economy and many others. On the physical ground, the periodicity itself can be associated either with space degrees of freedom such as in crystals, optical lattices and systems of ring topologies or with time-periodic drivings such as ac currents, magnetic or electric fields and rocking and pulsating forces to name but a few. It also can be present in both these domains. Typical realizations can range from biophysics [2] with the description of biomotors movement on asymmetric periodic microtubules [3] or transport inside ion channels [4], to the recent experiments with optical lattices [5, 6], quantum mesorings [7] or Josephson junctions [8].

The Josephson effect has been known for half a century [9]. So far it has been utilized for the definition of the voltage standard [10] or for more practical devices as elements in high-speed circuits [8] or even for future applications in quantum computing devices [11]. Surprisingly, after 50 years of intensive theoretical and experimental research, we are still able to find new and uncommon phenomena even in a simple system of two weakly connected superconductors. Recently, the counterintuitive phenomenon of absolute negative conductance (ANC) was reported in the single driven, resistively and capacitively shunted Josephson junction device subjected to both a time-periodic (ac) and a constant biasing (dc) current [12]. The ANC phenomenon has been confirmed by a suitable experiment with a Josephson junction setup [13] and, very recently, with ultracold atoms in optical lattices [6]. Other aspects of anomalous transport phenomena such as the occurrence of a negative differential conductance and the emergence of a negative nonlinear conductance in the non-equilibrium response regime remote from zero dc bias have been studied in a series of papers [14]. The influence of the unbiased biharmonic ac current on a single junction has been considered in [15]. In recent years, the dynamics of the phase difference of coupled junctions has been addressed [16, 17].

This paper is organized as follows. In section 2, we present the model of two interacting junctions. Next, in section 3, the numerical investigation of transport properties for two scenarios (A) and (B) of drivings applied to two coupled junctions is compared. The paper ends with a summary and conclusions in section 4.

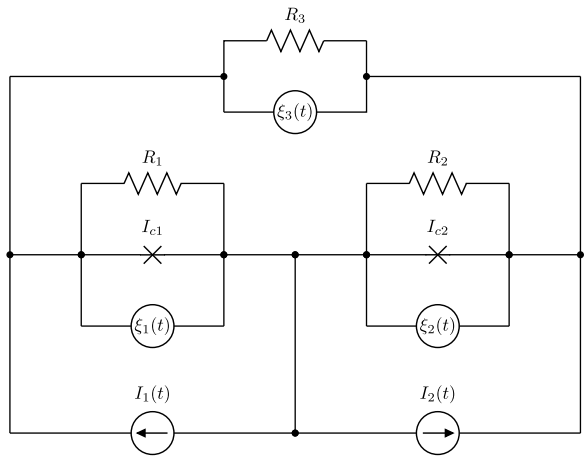

Figure 1. The system of two coupled Josephson junctions characterized by the critical Josephson supercurrents (I_{c1}, I_{c2}), resistances (R_1, R_2), shunted by the external resistance R_3, influenced by the Johnson–Nyquist thermal noise sources $(\xi_1(t),\ \xi_2(t),\ \xi_3(t))$ and driven by the external currents $(I_1(t), I_2(t))$.

2. Model of driven interacting junctions

From a more general point of view, we explore the system consisting of two subunits (subsystems) interacting with each other. The system is driven out of its equilibrium state by an external force. As a particular realization of this idea we propose two resistively shunted Josephson junction devices characterized by the critical Josephson supercurrents (I_{c1}, I_{c2}), resistances (R_1, R_2) and phases (ϕ_1, ϕ_2) [18]. A schematic circuit representing the model is shown in figure 1. The system is externally shunted by the resistance R_3 and driven by two current sources $I_1(t)$ and $I_2(t)$ acting on the first and the second junction, respectively. We include in the model the Johnson–Nyquist thermal noise sources $\xi_1(t)$, $\xi_2(t)$ and $\xi_3(t)$ associated with the corresponding resistances R_1, R_2 and R_3 according to the fluctuation–dissipation theorem.

The beauty of the standard Josephson theory lies in the simplicity of the model. In the semiclassical regime, when the spatial dependence of characteristics can be neglected and photon-assisted tunnelling phenomena do not contribute, the so-called Stewart–McCumber model [19] holds true (for an extensive discussion on the validity of the model, see [10]). In this regime, one can use the classical Kirchhoff current and voltage laws, and two Josephson relations to derive two evolution equations for the phases $\phi_1 = \phi_1(t)$ and $\phi_2 = \phi_2(t)$. The dimensional version of the equations is presented in [17]. Here, we recall their dimensionless form, namely

$$\dot{\phi}_1 = I_1(\tau) - I_{c1}\sin\phi_1 + \alpha[I_2(\tau) - I_{c2}\sin\phi_2] + \sqrt{D}\,\eta_1(\tau), \tag{1a}$$

$$\dot{\phi}_2 = \alpha\beta[I_2(\tau) - I_{c2}\sin\phi_2] + \alpha[I_1(\tau) - I_{c1}\sin\phi_1] + \sqrt{\alpha\beta D}\,\eta_2(\tau), \tag{1b}$$

where $\phi_i = \phi_i(\tau)$ for $i = 1, 2$ and the dot denotes a derivative with respect to the dimensionless time τ expressed by the dimensional time t as

$$\tau = \frac{2eV_0}{\hbar}t, \quad V_0 = I_c\frac{R_1(R_2+R_3)}{R_1+R_2+R_3}, \quad I_c = \frac{I_{c1}+I_{c2}}{2}. \tag{2}$$

The parameters

$$\alpha = \frac{R_2}{R_2+R_3} \in [0,1], \quad \beta = 1+\frac{R_3}{R_1}, \quad D = \frac{4ek_BT}{\hbar I_c}. \tag{3}$$

All dimensionless currents $I_1(\tau)$, $I_2(\tau)$, I_{c1} and I_{c2} are in units of I_c, e.g. $I_{c1} \to I_{c1}/I_c$. Thermal equilibrium noise sources related to the resistances R_1, R_2 and R_3 are modelled here by the independent δ-correlated zero-mean Gaussian white noises $\xi_i(t)$ $(i = 1, 2, 3)$, i.e. $\langle\xi_i(t)\xi_j(s)\rangle = \delta_{ij}\delta(t-s)$ for $i, j \in \{1, 2, 3\}$. The straightforward assumption of identical temperature T felt by all parts of the setup allows for the reduction of the number of original noises ξ_1, ξ_2 and ξ_3 (see figure 1) to their linear combination η_1 and η_2 in equations (1*a*) and (1*b*).

The reader would find it easier to understand this scenario within a pure mechanical picture. The dynamics of the phase difference can be mapped onto the motion of the Brownian particle. In this mechanical analogue the correspondence between position x_1 of the first particle with the phase difference ϕ_1 of the first junction can be settled and the position x_2 of the second particle can mimic the phase difference ϕ_2 of the second junction. If we imagine two interacting particles moving along the periodic structure, then the most significant quantifiers describing their transport properties would be the average velocities of the first $v_1 = \langle\dot{\phi}_1\rangle$ and the second $v_2 = \langle\dot{\phi}_2\rangle$ particle, respectively. In terms of the Josephson junction system it corresponds to the dimensionless long-time averaged voltages $v_1 = \langle\dot{\phi}_1\rangle$ and $v_2 = \langle\dot{\phi}_2\rangle$ across the first and second junctions, respectively (from the Josephson relation, the dimensional voltage $V = (\hbar/2e)\mathrm{d}\phi/\mathrm{d}t$ and therefore $\mathrm{d}\phi/\mathrm{d}\tau = V/V_0$). The junction resistances (or conductance) translate then into the particles mobility. Moreover, the phase space of the deterministic system is three dimensional $\{\phi_1(\tau), \phi_2(\tau), \omega\tau\}$ and therefore gives rise to possible chaotic evolution, which is a key feature of anomalous transport [12, 14, 20].

2.1. Identical junctions

Without loss of generality, we can reduce a number of parameters assuming that two junctions are *identical* to $R_1 = R_2$ and $I_{c1} = I_{c2} \equiv 1$. In such a case, $\alpha\beta = 1$ and equations (1*a*) and (1*b*) take the symmetric form

$$\dot{\phi}_1 = I_1(\tau) - \sin\phi_1 + \alpha[I_2(\tau) - \sin\phi_2] + \sqrt{D}\,\eta_1(\tau), \tag{4a}$$

$$\dot{\phi}_2 = I_2(\tau) - \sin\phi_2 + \alpha[I_1(\tau) - \sin\phi_1] + \sqrt{D}\,\eta_2(\tau). \tag{4b}$$

The parameter $\alpha = R_2/(R_2+R_3) \in [0, 1]$ plays the role of coupling strength between the junctions and can be tuned by the variation of the external resistance R_3. When $\alpha = 0$ the set of equations (4) decouple into two independent equations. It can be realized by taking $R_3 \to \infty$. The opposite situation with two fully coupled junctions can be worked out by designating $R_3 = 0$. The noise strength D can be tuned

by the temperature. The currents $I_1(\tau)$ and $I_2(\tau)$ are energy sources pumped into the system and can be applied to one or to both the junctions.

2.2. External current driving

A trivial way of inducing the dc voltage across both the junctions is to apply the dc current to both the junctions separately (in the mechanical analogue, it corresponds to the static force). It appears that we can also achieve it by applying the dc current to only one junction, but we have to make sure that coupling is strong enough to call out the response on the other junction too. This, however, seems to be rather uninteresting and a well-known solution. What if we abandon simple intuitive possibilities? We can exploit the well-known ratchet effect [21] and induce the non-zero dc voltage by applying a zero-mean external current. We consider two scenarios. In the first scenario (A), the ac driving is to be applied to only one of the junctions [15, 17], namely

$$I_1(\tau) = a_1 \cos(\omega\tau) + a_2 \cos(k\omega\tau + \theta), \quad I_2(\tau) = 0, \tag{5}$$

where θ is the relative phase between the driving currents and k is a real number.

In the second scenario (B), the external current is split into two simple harmonic components applied to two respective junctions, namely

$$I_1(\tau) = a_1 \cos(\omega\tau), \quad I_2(\tau) = a_2 \cos(k\omega\tau + \theta). \tag{6}$$

We know that the symmetric driving cannot itself induce the non-zero dc voltage. However, we expect that the coupling between junctions would have to play a crucial role in the dynamics of the total system and a non-zero dc voltage could be generated for $\alpha > 0$. We ask which of the two scenarios (5) or (6) is more efficient in the sense that the induced dc voltages have greater amplitudes. In method (5), we have the possibility to induce the non-zero dc voltage just by the ratchet effect, cf the detailed discussion in [17]. In this case, even for $\alpha = 0$ we still can find non-zero dc voltage across the first junction. In scenario (6), the separated symmetric ac currents cannot alone induce non-zero voltage in the decoupled junctions. Setting the parameter $\alpha \neq 0$, we effectively incorporate the ratchet effect and in turn create a prospect of dc transport in the system.

3. dc voltage characteristics

Stochastic differential equations (4) cannot be handled by known analytical methods. For this reason we have carried out extensive numerical simulations. We have used the second-order Stochastic Runge–Kutta algorithm with the time step of about $10^{-3} \times (2\pi/\omega)$. The initial phases $\phi_1(0)$ and $\phi_2(0)$ have been randomly chosen from the interval $[0, 2\pi]$. Averaging was performed over 10^3–10^6 different realizations and over one period of the external driving $2\pi/\omega$. Numerical simulations have been carried out using the CUDA environment on the desktop computing processor NVIDIA GeForce GTX 285. This gave us the possibility to speed up the numerical calculations up to a few hundreds of times more than on typical modern CPUs [22]. Below, we present the results for a fixed frequency multiplier $k = 2$. This will reflect the typical biharmonic driving studied previously for Hamiltonian systems [23], systems in the overdamped regime [24, 25] and for the moderate damping [26, 27]. If the given parameter is not addressed directly in the plot, we will keep the constant values as follows: the noise strength (or equivalently the dimensionless temperature) $D = 0.001$, the frequency of the ac driving $\omega = 0.039\,44$, the coupling strength $\alpha = 0.56$, the relative phase $\theta = \pi/2$ and the amplitudes $a_1 = a_2 = 1$.

In the long-time limit, the averaged voltages $\langle\dot{\phi}_i(\tau)\rangle$ can be presented in the form of a series of all possible harmonics, namely

$$\lim_{\tau\to\infty} \langle\dot{\phi}_i(\tau)\rangle = v_i + \sum_{n=1}^{\infty} v_i(n\omega\tau), \quad i = 1, 2, \tag{7}$$

where v_i is a dc (time-independent) component and $v_i(n\omega t)$ are time-periodic functions of zero average over a basic period. For high frequency ω (i.e. fast alternating currents) the averaged dc voltages are zero: very fast positive and negative changes in the driving current cannot induce the dc voltage and only multi-harmonic components of the voltages can survive. In addition, if both amplitudes a_1, a_2 are smaller than the critical supercurrents, then from the structure of the model (4) it follows that the net voltage will be zero or very close to zero.

In figure 2, the long-time averaged dc voltages across the first (v_1) and second (v_2) junctions are shown in the amplitude parameter plane $\{a_1, a_2\}$. There is clearly zero average voltage for small values of both amplitudes. However, for larger amplitudes in both scenarios (5) and (6) we can recognize four operating regimes where

(i) $v_1 > 0$ and $v_2 > 0$,
(ii) $v_1 < 0$ and $v_2 < 0$,
(iii) $v_1 < 0$ and $v_2 > 0$,
(iv) $v_1 > 0$ and $v_2 < 0$.

Of course, the quantitative picture is different. One can easily see that in the case of (5), the transport properties of the first (driven) junction have a more complicated strips-like structure with a larger area of negative voltage. For the second (non-driven) junction, the dc voltage v_2 can be two to three times greater than v_1. On the other hand, in the case of (6), the regimes of negative voltage are smaller. We emphasize that such complicated regimes of islands and tongues of negative and positive dc voltages are not just rare occurrences: they can be verified with numerically arbitrarily high-accuracy calculations and over extended intervals in the parameter space.

In figure 3, we have selected the region where for the scenario (5) the dc voltage on the first (driven) junction stays negative or zero (more precisely, so small as to be negligible) throughout the presented range of both amplitudes. The second (non-driven) junction shows all possible working states with the negative, positive and zero dc voltage (see the left panels of figure 3). In the same region but for the second scenario (6), the first junction driven by the current $\cos\omega\tau$ stays positive for all presented values of both current

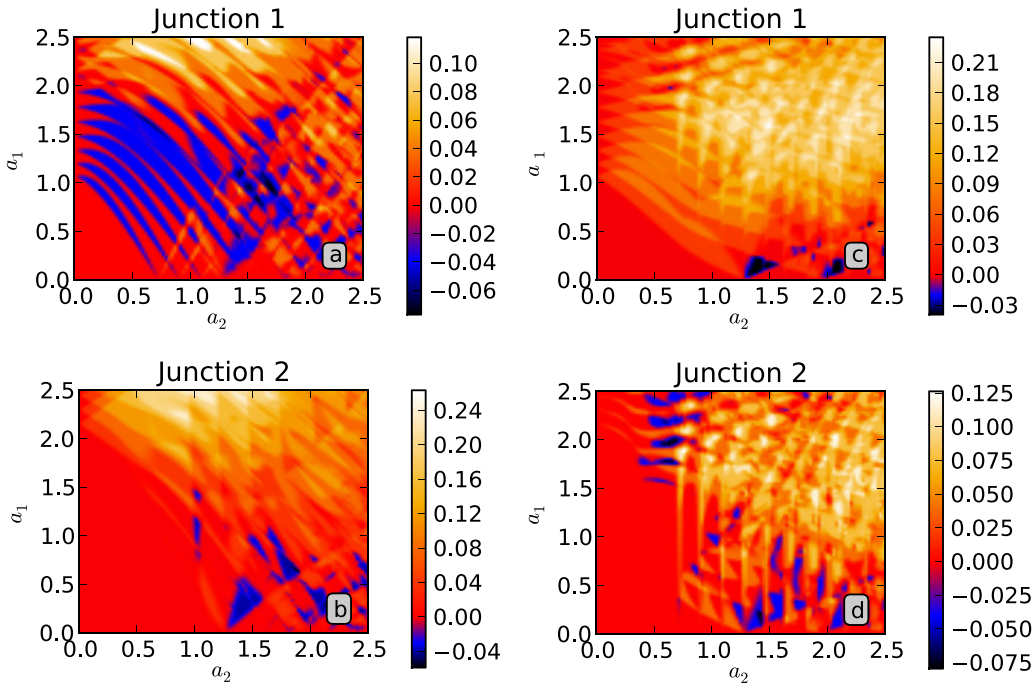

Figure 2. The stationary averaged dc voltages v_1 and v_2 across the first and the second junction. The dependences on the external ac current amplitudes a_1 and a_2 are presented in panels (a) and (b) for the driving (5) acting on the first junction only and in panels (c) and (d) for the driving (6) split between two junctions. Other parameters read as: the dimensionless temperature $D = 0.001$, the frequency $\omega = 0.039\,44$, the coupling strength $\alpha = 0.56$, the relative phase $\theta = \pi/2$ and the frequency multiplier $k = 2$.

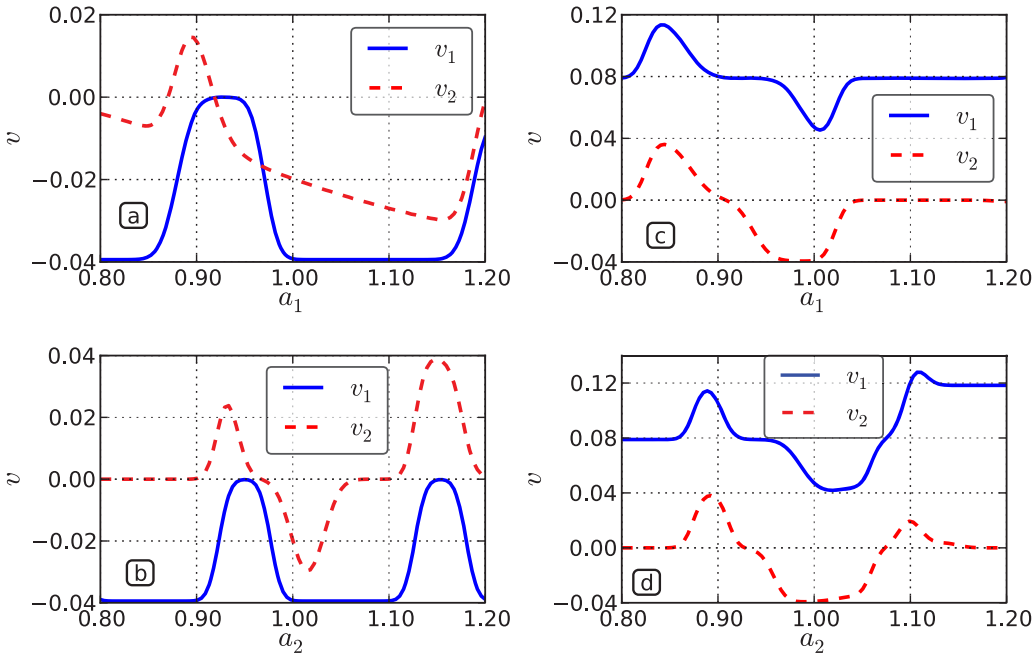

Figure 3. The stationary averaged dc voltages v_1 and v_2 across the first (—— blue line) and the second (- - - - red line) junction, respectively. The dependences on the external ac current amplitudes a_1 and a_2 are presented for the driving (5) in panels (a) and (b) and for the driving (6) in panels (c) and (d). The other parameters read as: the dimensionless temperature $D = 0.001$, the frequency $\omega = 0.039\,44$, the coupling strength $\alpha = 0.56$, the relative phase $\theta = \pi/2$ and the frequency multiplier $k = 2$ and the amplitudes $a_1 = a_2 = 1$.

amplitudes a_1 and a_2, while the junction driven by the current $\cos(2\omega\tau + \pi/2)$ can assume positive and negative values. What is also striking is that in the case of (6) the voltage characteristics of both junctions change with some synchrony: the voltages increase or decrease when one of the current amplitudes varies. This feature, in turn, is not found in scheme (5).

As the next point of analysis, we ask about the role of thermal fluctuations. It is presented in the upper panels of figure 4. In this regime we can note the voltage reversal [28] across the second junction: the voltage v_2 can change its sign from negative to positive values when the temperature is increased. On the other hand, the voltage v_1 is always negative for scenario (5) and is always positive for scenario (6).

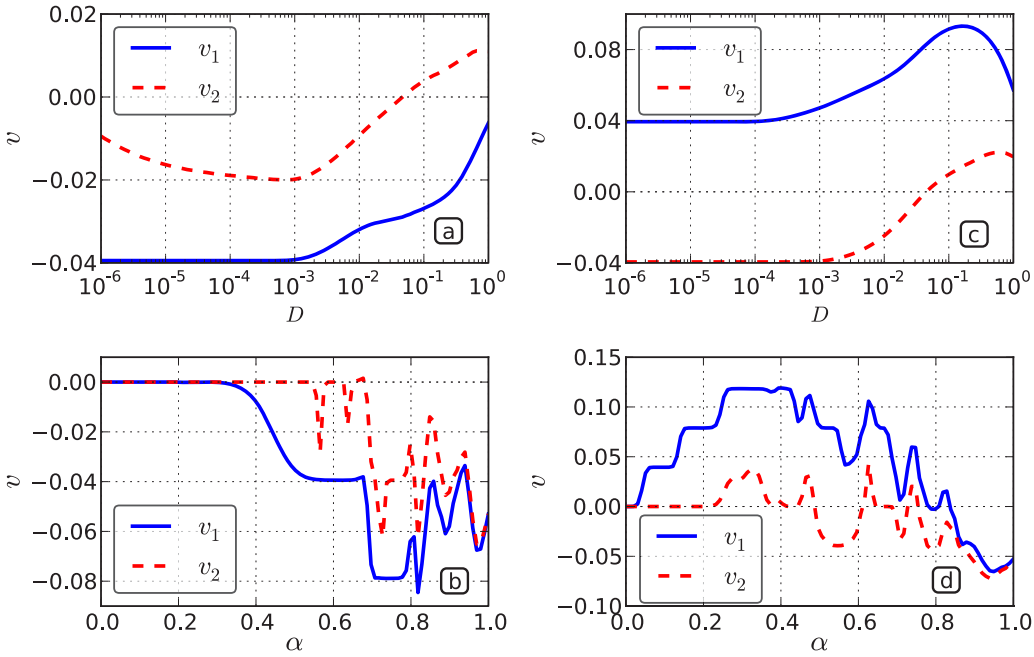

Figure 4. The stationary averaged dc voltages v_1 and v_2 across the first (—— blue line) and the second (- - - - red line) junction, respectively. The dependences on the noise strength (or dimensionless temperature) D (upper panels) and on the coupling strength α (lower panels) are presented for the driving (5) in panels (a) and (b) and for the driving (6) in panels (c) and (d). The other parameters if not addressed directly in the plots read as: the dimensionless temperature $D = 0.001$, the frequency $\omega = 0.039\,44$, the coupling strength $\alpha = 0.56$, the relative phase $\theta = \pi/2$, the current amplitudes $a_1 = a_2 = 1$ and the frequency multiplier $k = 2$.

For high temperature, both voltages tend to zero. Next, we address the issue of whether, and to what extent, the coupling strength α can influence voltage properties. The results are depicted in the bottom panels of figure 4. The first note is a non-monotonic and irregular dependence of both voltages on α with several minima and maxima. In scenario (6), a step-like dependence of the voltage across the first junction is observed for small values of the coupling α.

4. Summary

In this study we numerically analysed the role of ac current drivings on the transport properties of resistively shunted two coupled Josephson junctions. We identified a rich variety of dc voltage characteristics in the parameter space where transport can be experimentally monitored. We have detected regions displaying positive and negative dc voltages, which form complicated structures in the parameter space. We have mainly focused the analysis on impact of selected regimes in the parameter space on voltage properties. Other regimes of parameters also modify voltage characteristics but here we do not present all varieties. A general observation is that in the same parameters regimes, the biharmonic ac driving applied to only one junction results in a smaller dc voltage than in the case when the ac current is split into two simple harmonics and each is applied to the respective junctions.

Acknowledgment

The work was supported in part by grant no. N202 052940 and the ESF Program ‘Exploring the Physics of Small Devices’.

References

[1] Łuczka J, Bartussek R and Hänggi P 1995 *Europhys. Lett.* **31** 431
[2] Neimann A, Hänggi P, Jung P and Schimansky-Geier L (ed) 2004 Special issue on noise in biophysical systems *Fluctuation Noise Lett.* **4** Issue 1
[3] Astumian R D 2002 *Sci. Am.* **285** 56
Astumian R D and Hänggi P 2002 *Phys. Today* **55** 33
[4] Burada P S, Schmid G, Talkner P, Hänggi P, Reguera D and Rubi J M 2008 *Biosystems* **93** 16
[5] Renzoni F 2005 *Contemp. Phys.* **46** 161
[6] Salger T, Kling S, Denisov S, Ponomarev A V, Hänggi P and Weitz M 2012 arXiv:1202.5174v1
[7] Bluhm H, Koshnick N C, Bert J A, Huber M E and Moler K A 2009 *Phys. Rev. Lett.* **102** 136802
Machura L, Rogoziński S and Łuczka J 2010 *J. Phys.: Condens. Matter* **22** 422201
[8] Barone A and Paternò G 1982 *Physics and Application of the Josephson Effect* (New York: Wiley)
[9] Josephson B D 1962 *Phys. Lett.* **1** 251
Josephson B D 1964 *Rev. Mod. Phys.* **36** 216
[10] Kautz R L 1996 *Rep. Prog. Phys.* **59** 935
[11] Makhlin Y, Schön G and Shnirman A 2001 *Rev. Mod. Phys.* **73** 357
Mariantoni M *et al* 2011 *Nature Phys.* **7** 287
[12] Machura L, Kostur M, Talkner P, Łuczka J and Hänggi P 2007 *Phys. Rev. Lett.* **98** 040601
[13] Nagel J, Speer D, Gaber T, Sterck A, Eichhorn R, Reimann P, Ilin K, Siegel M, Koelle D and Kleiner R 2008 *Phys. Rev. Lett.* **100** 217001
[14] Kostur M, Machura L, Hänggi P, Łuczka J and Talkner P 2006 *Physica* A **371** 20
Machura L, Kostur M, Talkner P, Hänggi P and Łuczka J 2010 *Physica* E **42** 590
Kostur M, Machura L, Talkner P, Hänggi P and Łuczka J 2008 *Phys. Rev.* B **77** 104509
Kostur M, Machura L, Łuczka J, Talkner P and Hänggi P 2008 *Acta Phys. Pol.* B **39** 1115

[15] Machura L, Kostur M and Łuczka J 2010 *Chem. Phys.* **375** 445
Machura L and Łuczka J 2010 *Phys. Rev.* E **82** 031133
[16] Januszewski M and Łuczka J 2011 *Phys. Rev.* E **83** 051117
[17] Machura L, Spiechowicz J, Kostur M and Łuczka J 2012 *J. Phys.: Condens. Matter* **24** 085702
[18] Nerenberg M A H, Blackburn J A and Jillie D W 1980 *Phys. Rev.* B **21** 118
[19] Stewart W C 1968 *Appl. Phys. Lett.* **12** 277
McCumber D E 1968 *J. Appl. Phys.* **39** 3113
[20] Speer D, Eichhorn R and Reimann P 2007 *Europhys. Lett.* **79** 10005
[21] Łuczka J 1999 *Physica* A **274** 200
Hänggi P and Marchesoni F 2009 *Rev. Mod. Phys.* **81** 387
[22] Januszewski M and Kostur M 2010 *Comput. Phys. Commun.* **181** 183
[23] Flach S, Yevtushenko O and Zolotaryuk Y 2000 *Phys. Rev. Lett.* **84** 2358
[24] Borromeo M, Hänggi P and Marchesoni F 2005 *J. Phys.: Condens. Matter* **17** S3709
Chenggui Yao, Yan Liu and Meng Zhan 2011 *Phys. Rev.* E **83** 061122
[25] Yevtuschenko O, Flach S, Zolotaryuk Y and Ovchinnikov A A 2001 *Europhys. Lett.* **54** 141
[26] Wonneberger W and Breymayer H J 1981 *Z. Phys.* B **43** 329
Breymayer H J 1984 *Appl. Phys.* A **33** 1
[27] Machura L, Kostur M and Łuczka J 2010 *Chem. Phys.* **375** 445
Machura L and Łuczka J 2010 *Phys. Rev.* E **82** 031133
Cubero D, Lebedev V and Renzoni F 2010 *Phys. Rev.* E **82** 041116
[28] Kostur M and Łuczka J 2001 *Phys. Rev.* E **63** 021101